INVITED PAPER

Terahertz Time-Domain Spectroscopy for Material Characterization

The composition of glass and polymers, and the density and viscosity of lubricating oil, can be determined from the THz spectrographs of these materials.

By Mira Naftaly and Robert E. Miles, *Member IEEE*

ABSTRACT | Terahertz time-domain spectroscopy is used to study properties of nonpolar amorphous materials. Terahertz absorption spectra and refractive indices were measured in a number of glasses, lubricating oils, and polymers, and the results were correlated with material properties.

KEYWORDS | Amorphous materials; terahertz spectroscopy

I. INTRODUCTION

Coherent time-domain spectroscopy (TDS) using terahertz radiation [1]–[3] has been employed to look at a wide variety of materials, including ceramics [4], semiconductors [5], environmental pollutants [6], chemical mixtures [7], and gases [8]. Many of these materials were previously studied using far-infrared Fourier transform spectroscopy (FTS) in transmission and reflection modes. THz TDS differs from FTS in a number of important aspects [1]–[5] which give it some significant advantages. THz TDS uses coherent pulsed sources, typically of 1–2 ps duration; while FTS uses continuous-wave (CW) noncoherent sources. The TDS measurement is carried out in a pump–probe configuration, with the short probe pulse (< 0.1 ps) sweeping out the transient field of the THz pulse, giving a direct measurement of the field amplitude and phase. The THz spectrum is then obtained from the data by a Fourier transform. Since the absorption coefficient and the refractive index of the material studied are directly related to the amplitude and phase respectively of the transmitted field, both parts of the complex permittivity can be obtained by THz TDS. By contrast, FTS measures only the field intensity, and therefore provides only the absorption coefficient. Although the refractive index can be calculated from the FTS data by using Kramers–Krönig relations, the calculation is not straightforward and has many potential sources of error. As a further consequence of its coherent pump–probe detection scheme, TDS has a very high signal-to-noise ratio (SNR): typically $> 10^6$ in power, compared to $\sim$300 for FTS [5].

Moreover, the high-brightness, short-pulse sources used in THz TDS have peak optical intensities several orders of magnitude higher than the CW sources employed in FTS [5], allowing transmission studies to be carried out on materials with relatively high absorption coefficients. The frequency resolution of THz TDS can be as fine as $\sim$1 GHz, which is as good as the best of FTS instruments. However, the bandwidth of THz emitters is typically less than 5 THz, while that of FTS systems can extend into the near-infrared.

Terahertz spectroscopy studies fall into two categories: those aiming to identify or differentiate substances on the basis of their THz transmission spectra, and those focusing on the optical and dielectric properties of materials at terahertz frequencies. In the present paper we attempt to relate the data obtained by terahertz spectroscopy to the material properties. Nonpolar materials were chosen for the study, because of their relatively good transmission at THz frequencies enabling good quality data to be obtained. We describe the application of THz TDS to glasses, lubricating oils, and polymers. The measured terahertz absorption and refractive indices were correlated with material properties, and some relationships were identified. The results show the potential of

Manuscript received October 31, 2005; revised March 17, 2007. This work was supported by the Research Councils U.K. Basic Technology Research Programme.
The authors are with the School of Electronic and Electrical Engineering, University of Leeds, Leeds LS2 9JT, U.K. (e-mail: m.naftaly@leeds.ac.uk).
Digital Object Identifier: 10.1109/JPROC.2007.898835

terahertz spectroscopy as an experimental technique for material characterization.

II. EXPERIMENTAL

The THz TDS system, shown in Fig. 1, uses a 60 fs Ti–sapphire laser (Spectra-Physics Tsunami), employing a conventional configuration [1]–[3] for free-space THz generation and detection. The average power of the laser was 1.2 W, of which approximately 1.1 W was used for terahertz generation from a biased GaAs emitter. Electro-optic (EO) detection with balanced photodiodes was employed to observe the THz signal. The EO detector was a 1.5 mm thick ZnTe crystal cut so that the beam propagation was along its ⟨110⟩ axis. The use of a relatively thick ZnTe crystal increases the measured signal, although the obtainable bandwidth is reduced owing to crystal absorption and phase mismatch. However, this was not a problem, since the type of emitter employed was incapable of producing a significant amount of radiation at frequencies above 3 THz where the crystal absorption becomes significant. The dynamic range of the THz spectroscopy system was around 2000 in amplitude, and the usable bandwidth was from 100 GHz to 3 THz. The optical configuration was designed to provide a focused THz beam for imaging and a parallel beam for spectroscopy.

The emitter was fabricated on semi-insulating GaAs with an attached silicon hyperhemispherical lens [9]. It had parallel electrodes with a gap of 0.5 mm, and the applied bias was 200 V_{DC}. The average THz power, measured by a calibrated Golay detector, was approximately 50 μW. The emitted THz spectrum was obtained independently using a lamellar-mirror FTIR with a Golay detector, described in detail elsewhere [10]. The spectral profile obtained by the FTIR and the frequencies of the water absorption lines were found to agree with those measured by electrooptic detection, as shown in Fig. 2.

Absorption coefficients $a(\nu)$ and refractive indices $n(\nu)$ were calculated as a function of THz frequency ν from the sample and reference spectral data using equations [1]–[5]

$$\alpha(\nu) = -\ln\left[T(\nu)E_{sample}(\nu)/E_{reference}(\nu)\right]/d \quad (1)$$

$$n(\nu) = 1 + c\left[\phi_{sample}(\nu) - \phi_{reference}(\nu)\right]/[2\pi\nu d] \quad (2)$$

$$T(\nu) = 1 - R = 1 - [n(\nu) - 1]^2/[n(\nu) + 1]^2 \quad (3)$$

where E and ϕ refer respectively to the THz amplitude and phase, d is the sample thickness, and R the Fresnel loss at the air–sample interface.

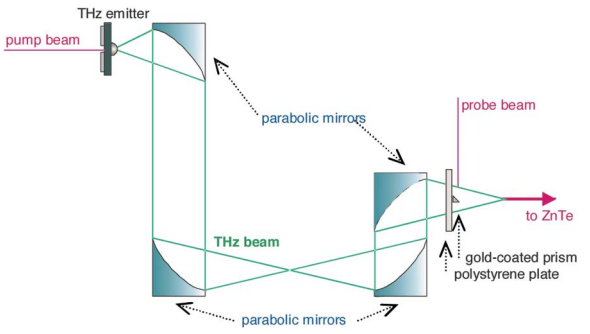

Fig. 1. *A schematic drawing of the THz TDS system.*

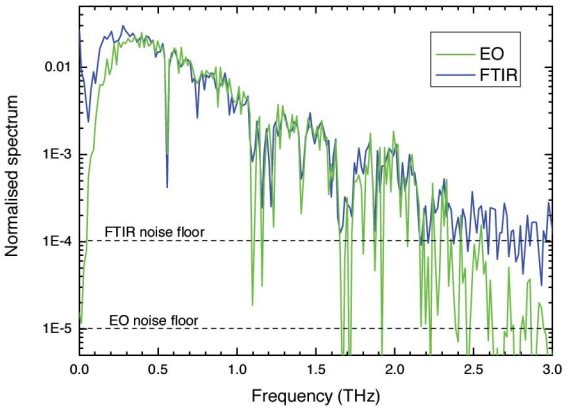

Fig. 2. *Comparison of the source THz spectra obtained using an FTIR and the TDS system (adjusted for losses in the ZnTe crystal). The TDS amplitude was squared in order to compare with the power spectrum from the FTIR. The sharp absorption peaks are due to water vapor, and provide a check of frequency accuracy.*

III. THz SPECTROSCOPY OF GLASSES

Glasses have infrared absorption spectra in the region stretching from around 10^4 cm^{-1} down to below 10 cm^{-1}. Over the years near- and far-infrared vibrational spectra of glasses have attracted a great deal of research interest, because they provide an insight into the glass structure and are closely related to the optical and mechanical properties. Vibrational modes in glasses have been investigated primarily by the techniques of Raman scattering [11], far-infrared transmission [12]–[14] and reflection spectroscopy [15], [16]. More recently THz absorption spectra and refractive indices have been obtained in a number of glasses and glass-ceramics [17], [18], demonstrating the potential usefulness of THz TDS for glass studies.

Commercially available optical flats were used in the study (Esco Products). The glasses were: polycrystalline fused quartz; amorphous fused silica; Pyrex (81% SiO_2, 13% B_2O_3, 4% Na_2O, 2% Al_2O_3); and BK7 (70% SiO_2, 11.5% B_2O_3, 9.5% Na_2O, 7.5% K_2O, 1.5 BaO). Absorption coefficients (α) and refractive indices (n) were obtained for each sample using (1)–(3). The values are plotted in

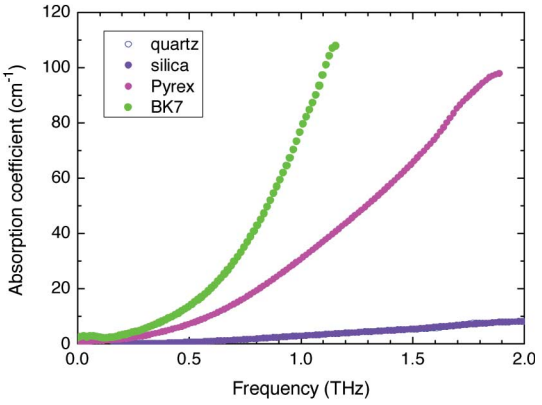

Fig. 3. *Absorption coefficients of the glasses studied, calculated using (1)–(3).*

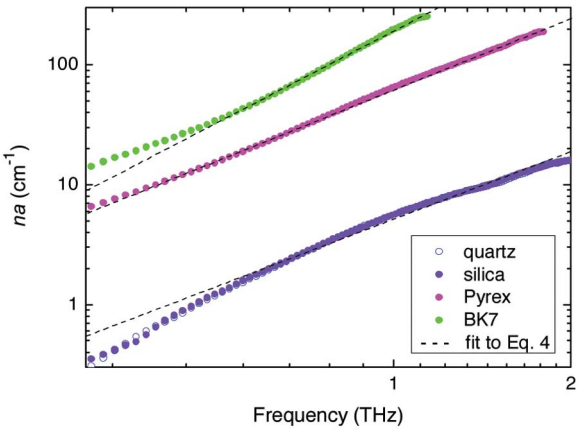

Fig. 5. *Frequency dependence of the product $n\alpha$ for the glasses studied, together with a fit to (4) (dashed line).*

Figs. 3 and 4. The spectral range of frequencies is narrower for Pyrex and BK7 glasses than it is for quartz and silica. This is because the dynamic range of the system limits measurement to the frequency band where transmission is 10^{-3} or higher. It is seen that THz absorption and refractive index in silica and quartz are identical, while those in Pyrex and BK7 differ significantly.

Figs. 3 and 4 show that THz absorption and refractive index in silica and quartz are relatively low, while the more ionic and highly disordered Pyrex and BK7 glasses have much stronger absorptions as well as higher refractive indices.

In simple terms, the increased THz absorption can be ascribed to the presence in Pyrex and BK7 glasses of ionic network modifiers (i.e., components which break up and modify the structure of the glass network) [19]. Of these, ionic alkali oxides especially increase the microscopic polarizability. This is confirmed by the fact that absorption in the high-alkali BK7 glass is much stronger than in low-alkali Pyrex.

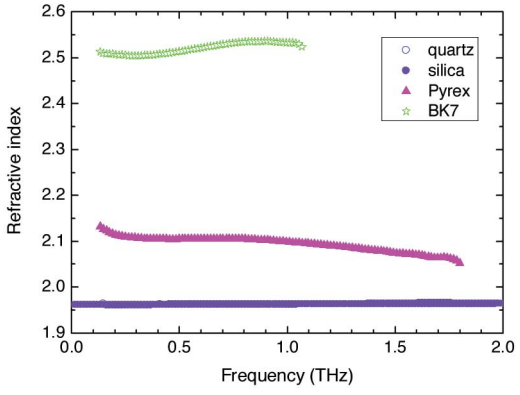

Fig. 4. *Refractive indices of the glasses studied, calculated using (1)–(3).*

Quantitatively, the effect of glass composition on THz transmission can be understood in the light of the relations [20], [21]:

$$n(\nu)\alpha(\nu) = K(h\nu)^{\beta} \tag{4}$$

where h is the Plank constant and β is an exponent which is approximately two in glassy materials. K is a factor which increases with the density of charge fluctuations in the material and with the refractive index. To verify this relationship, and to obtain the K and β parameters, Fig. 5 plots the product $n\alpha$ against frequency on a log-log scale; the dotted lines denote the fits to (4).

Fig. 5 shows the agreement between the data and the power relationship given by (4). The values of Kh^2 and β are listed in Table 1 (Kh^2 is given instead of K for easier comparison with Fig. 5). The value of β is 2.0 for quartz and silica, in agreement with the literature [20], [21]. In Pyrex the value of β is 1.9 and in BK7 it is 2.6, i.e., deviating from the theoretical value for amorphous materials. It is notable that the deviation from $\beta = 2$ is larger in the more disordered BK7 glass. The value of Kh^2 obtained for silica is 5 $\mathrm{cm^{-1}s^2}$, which is higher by a factor of two than that found by Strom *et al.* [20], [21]. However, the absorption coefficients (as shown in Fig. 3) agree with those quoted by other authors [12]–[14], [17], [18], while those given in [20] and [21] are smaller by a factor of 2. Thus the low value of absorption found in [20], [21] explains the discrepancy in the value of Kh^2.

Table 1 indicates two trends: that the values of both THz refractive index and of Kh^2 increase with the fraction of ionic network modifiers in the glass. Indeed Kh^2 is expected to increase with the refractive index [20], [21]; the relationship is shown in Fig. 6. Furthermore, the fact that Kh^2 increases with the proportion of alkali oxides indicates that it may be inversely related to the bonding

Table 1 THz Refractive Indices, and Kh^2 and B Parameters of Glasses

Glass	Fraction of network modifiers	Refractive index (average)	Kh^2 $cm^{-1}s^2$	β
Polycrystalline quartz	0	1.96±0.01	5±1	2.0±0.1
Amorphoussilica	0	1.96±0.01	5±1	2.0±0.1
Pyrex	6%	2.11±0.01	60±10	1.9±0.1
BK7	18.5%	2.52±0.01	190±30	2.6±0.1

strength in the glass. An indication of the bonding strength is provided by T_m, the glass melting temperature [22]. Such a relationship is indeed observed in Fig. 7, which plots Kh^2 against T_m (where the T_m values were obtained from the published data sheets).

It is of interest to note that the THz refractive indices of glasses are higher than in the visible, as shown in Fig. 8. That is because ionic polarizibility contributes to the dielectric constant of glasses at THz frequencies and below [23]. However, near the bandgap absorption in the UV, and in the mid-IR in the vicinity of phonon resonances, the refractive index increases on approaching an absorption edge or a resonance owing to anomalous dispersion [16]. An interesting feature of the data in Fig. 8 is that for these silicate glasses the THz refractive index appears to be linearly related to the visible refractive index.

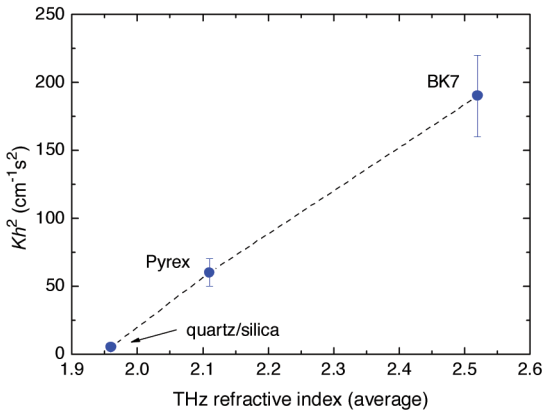

Fig. 6. *The relationship between the THz absorption coefficient Kh^2 and the average THz refractive index in the glasses studied.*

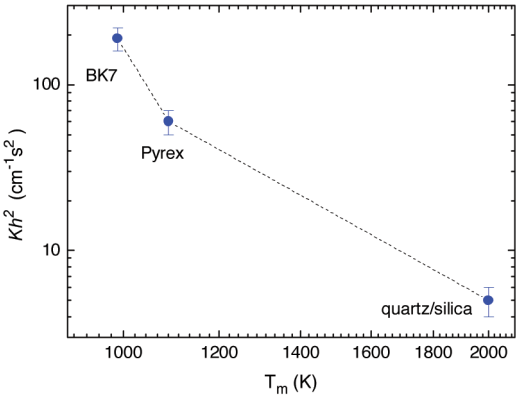

Fig. 7. *The relationship between the coefficient Kh^2 and the melting temperature T_m of the glasses studied.*

IV. THz SPECTROSCOPY OF LUBRICATING OILS

Infrared FTS has for many years been employed in the study of lubricating oils, their properties, and their interactions with surfaces [24]–[27]. Lubricating oils are also particularly suitable for study by THz TDS, since their absorbances in the far-infrared are relatively low and they also possess characteristic absorption features.

Two types of study were carried out. In the first, seven Shell lubricating oils, chosen so as to cover a wide range of types and properties, were examined. Information about the oils was provided by Shell UK; Table 2 lists the oils and some of their properties. The second study looked at changes in the transmission of car engine oil arising from prolonged use.

The sample cell employed in both studies had an optical path length of 3 cm, and was made of high-density polyethylene (HDPE) with a refractive index close to that of the oils (1.45).

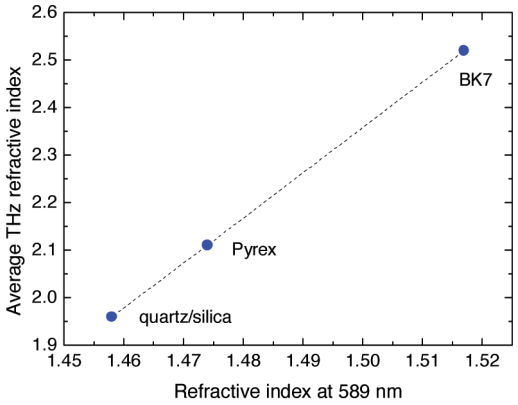

Fig. 8. *Comparison of refractive indices at THz and in the visible.*

Table 2 Shell Oils and Their Properties

Shell Oil (n/a = no additives w/a = with additives)	Pour point °C	Density @ 15°C g/cm^3	Viscosity @ 40°C cSt	THz refractive index
HVI 160, n/a, C20-C50	-9	0.893	30.8	1.486
HVI 650, n/a, >C25	-9	0.910	492	1.496
MVI 40, n/a, C15-C30	-39	0.873	8.6	1.475
Tellus R5, w/a	-40	0.850	5	1.467
Tellus 46, w/a	-30	0.870	46	1.481
Tonna S68, w/a	-30	0.885	68	1.484
Risella MH, refined	-	0.865	68	1.478

Fig. 9 plots THz absorption in the Shell oils: the additive-free oils are shown in Fig. 9(a); the additive-containing oils are shown in Fig. 9(b); and Fig. 9(c) compares different types of oil. It is seen that all seven oils show a steep rise in absorption with frequency. This behavior, seen in many amorphous materials, can be caused by the coupling of radiation into the acoustic phonon modes of the material [8]. In Fig. 9(a) and 9(b) pairs of similar type of oil (HVI 160 & 650; Tellus R5 & 46) are seen to have similar THz absorption curves, i.e., THz absorption is only weakly affected by the length of hydrocarbon chains in the oil or by its viscosity. By contrast, oils with different compositions, due either to additives or to a different refining process, have markedly different absorption curves. Fig. 9(c) compares three light oils of different compositions (HVI 160, Tellus R5, MVI 40) and the highly purified Risella MH oil. It is seen that variations in oil compositions give rise to changes in the THz absorption spectra. Notably the purified Risella oil has the lowest and most featureless absorption curve. These results suggest that lubricating oil compositions can be analyzed and/or monitored by THz spectroscopy.

The THz refractive indices of oils are listed in Table 2; since all oils exhibit negligible dispersion, a single value is given. It can be observed that the THz refractive indices correlate with both the density and viscosity of the oil. This is shown in Fig. 10, where different symbols are used to denote oils with and without additives and the purified oil Risella. It is seen that for both additive-containing and additive-free oils, a nearly linear relationship appears to exist between the THz refractive index and: i) the density [Fig. 10(a)] and ii) the logarithm of viscosity [Fig. 10(b)]. However, Risella oil deviates significantly from the common trend. It may be revealing to consider that both the density and viscosity of oils increase with the length of the hydrocarbon chains, and that therefore their THz refractive index may be related to the chain length or molecular weight.

It is of interest to note that THz transmission data provide information on both the composition and mechanical properties of oils: the absorption spectra are

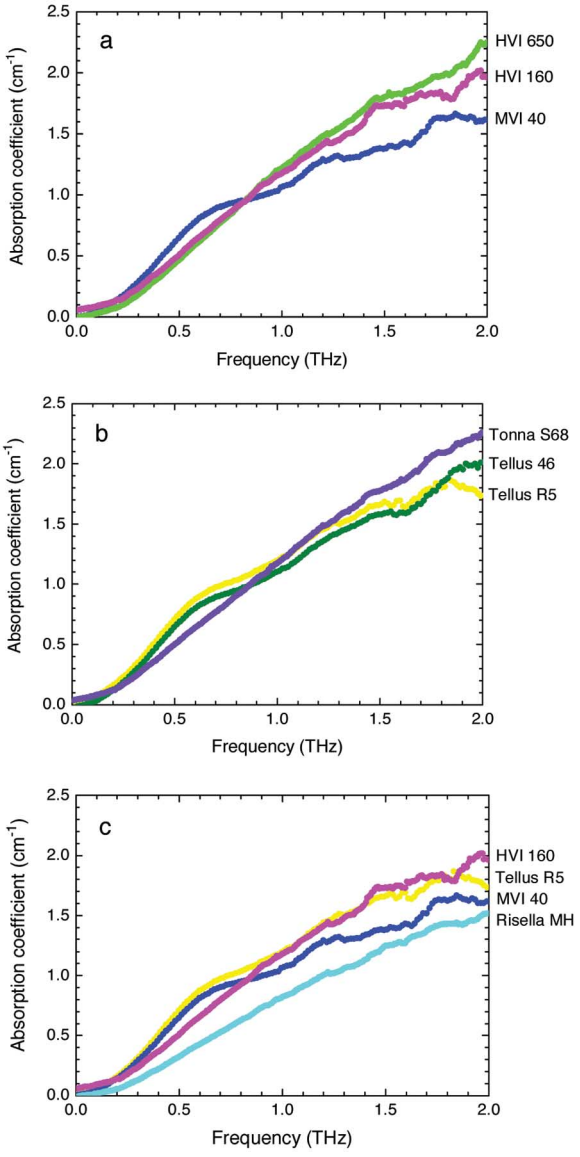

Fig. 9. *THz absorption in the Shell oils. (a) Additive-free oils. (b) Additive-containing oils. (c) Comparison of different types of oil.*

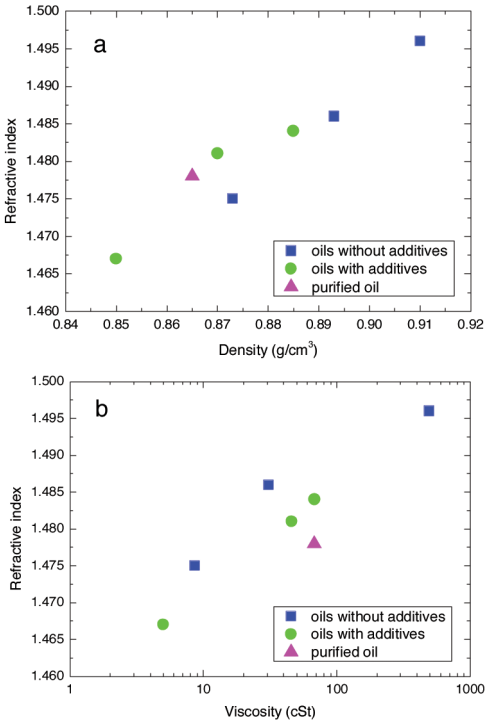

Fig. 10. *THz refractive indices versus: (a) oil density and (b) oil viscosity.*

dependent on oil composition; while the refractive indices correlate with density and viscosity.

In another set of experiments, THz transmission of a car engine oil was examined at different stages of use: clean unused oil; oil after six months of use; and overused oil after three years of use. The transmission spectra are shown in Fig. 11; the refractive index remained constant at 1.5. But it is seen that THz absorption increases with the extent of oil use, possibly indicating oil deterioration and/or contamination, and offering a useful tool for oil testing. Scattering is unlikely to have contributed to the increased loss, since the oil was free of sufficiently large particles.

V. THz SPECTROSCOPY OF POLYMERS

Far-infrared transmission in polymers has long been of interest both to materials research and for applications in submillimeter-wave technologies. Numerous studies have been carried out using FTS [28]–[31], and more recently THz TDS [32]–[35]. Here we look at two types of polymer studies: i) observing changes in THz transmission which occur during the polymerization process and ii) examining different types of polymers both for characterization purposes and in order to relate THz transmission to material properties.

The first study examined cross linking in SU8, which is a three-component curable epoxy resin widely used as an

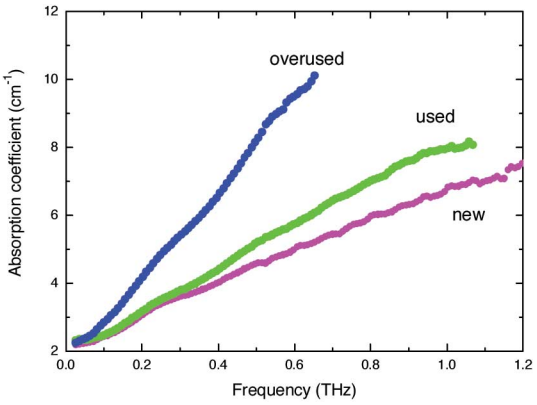

Fig. 11. *THz transmission of a car engine oil at various stages of use.*

ultrathick negative photoresist [32]. The resin is usually deposited by spin-coating onto a substrate, which for this work was chosen to be TPX owing to its good THz transparency [29]. The resin is cured by exposure to UV light, causing formation of cross-linkages.

An SU8 sample was prepared by spin-coating a 1-mm-thick layer onto a TPX substrate. The transmission properties of the uncured sample were measured immediately following deposition. The sample was then fully cured, and its transmission properties were measured again.

The results, seen in Figs. 12 and 13, show that there is a significant decrease in both THz absorption and refractive index resulting from the curing process. Since SU8 is optically transparent, the difference cannot be attributed to scattering. It is also of interest that, unlike other amorphous materials studied here, SU8 exhibits strong dispersion.

Four types of polymer sheets, obtained from commercial suppliers, were studied, all of which are highly transparent in the THz range. These were HDPE (high-density polyethylene), polystyrene, polycarbonate, and

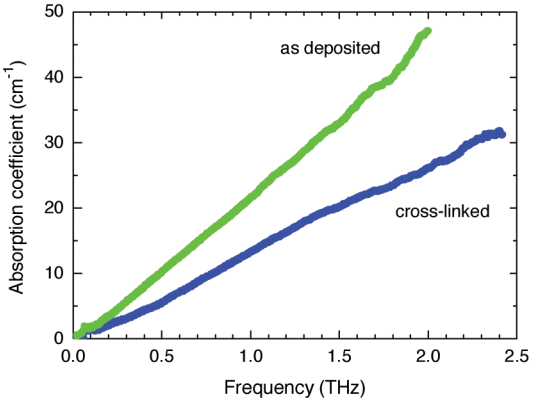

Fig. 12. *THz absorption in uncured and cured SU8.*

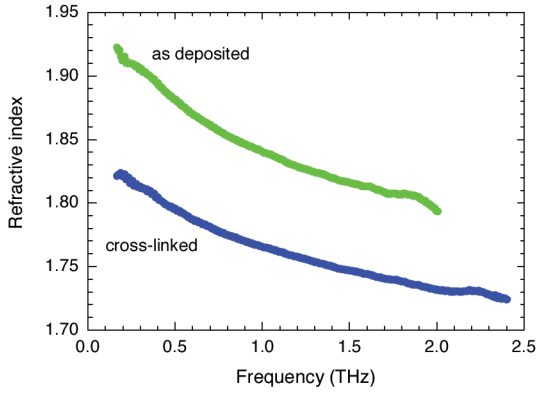

Fig. 13. *THz refractive index in uncured and cured SU8.*

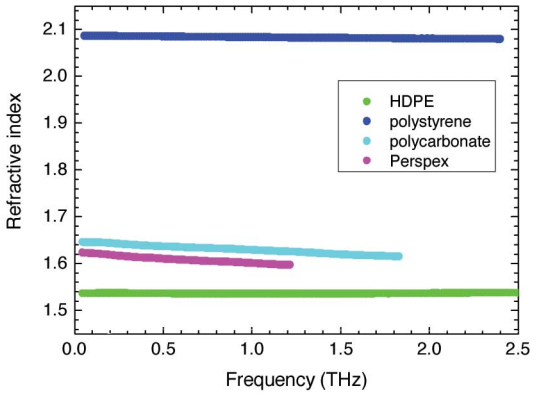

Fig. 15. *THz refractive index in HDPE, polystyrene, polycarbonate and Perspex.*

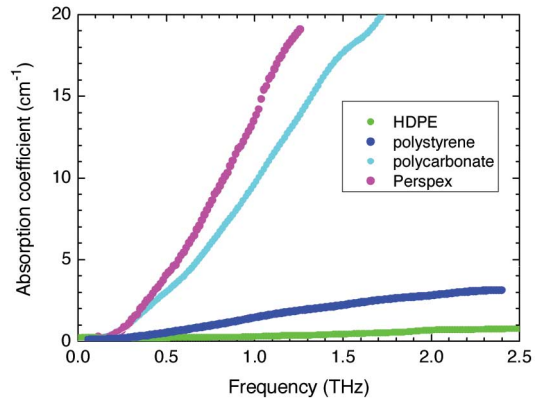

Fig. 14. *THz absorption in HDPE, polystyrene, polycarbonate and Perspex.*

Table 3 THz Refractive Indices and Kh^2 and B Parameters of Polymers

Polymer	Refractive index (average)	Kh^2 $cm^{-1}s^2$	β
HDPE	1.54±0.01	0.20 ±0.05	1.9±0.1
polystyrene	2.08±0.01	1.5±0.3	1.7±0.1
polycarbonate	1.63±0.01	19±3	1.9±0.1
Perspex	1.61±0.01	23±3	1.9±0.1
SU8 uncured	1.87±0.1	40±4	1.0±0.1
SU8 cured	1.79±0.1	26±3	0.9±0.1

Perspex (polymethyl methacrylate or PMMA). Figs. 14 and 15 show respectively the THz transmission spectra and refractive indices of the samples. The values for HDPE, polycarbonate, and Perspex are similar to those reported in [35]. It is seen that polymers are strongly differentiated by their THz absorption and refractive indices. Table 3 lists the average refractive indices and the Kh^2 and β absorption parameters.

Considering the data in Table 3, it is seen that the four polymer sheets conform to the power law dependence of absorption on frequency, as described by (4). The exponent β in these polymers is close to 2, confirming their glassy nature. In this they contrast with SU8, where THz absorption in both uncured and cured samples exhibits a near-linear frequency dependence. The value of β in Perspex (PMMA) agrees with that given in [20], [21]; however, the value of Kh^2 is larger by a factor of two than that in [20], [21], which may be explained similarly as in the case of silica (Section III). Unlike in glasses, there is no correlation between the absorption parameter Kh^2 and the THz refractive index. This may be attributed to the fact that the four polymers studied have very different chemical compositions and properties, unlike the three glasses studied in Section III, which all belong to the silicate family.

VI. CONCLUSION

THz TDS was used to study glasses, lubricating oils, and polymers. Relationships were observed between the composition and structure of the studied materials and their THz absorption spectra and refractive indices. THz absorption in glasses was seen to conform to the square law behavior, and to increase with the fraction of network modifiers in the composition. In lubricating oils, the THz refractive index was found to increase with oil density and viscosity; while THz absorption was related to the oil composition, and was seen to increase with use in car engine oil. In an epoxy resin THz absorption was seen to decrease following polymerization; whilst in four polymers THz absorption and refractive index were found to be strongly differentiated. THz TDS was therefore shown to be a valuable tool in the study of materials. ■

Acknowledgment

The authors wish to acknowledge the assistance of Shell UK in providing data sheets of its lubricating oils.

REFERENCES

[1] M. C. Beard, G. M. Turner, and C. A. Schmuttenmaer, "Terahertz spectroscopy," *J. Phys. Chem B*, vol. 106, pp. 7146–7159, 2002.

[2] M. Hangyo, T. Nagashima, and S. Nashima, "Spectroscopy by pulsed terahertz radiation," *Meas. Sci. Technol.*, vol. 13, pp. 1727–1738, 2002.

[3] P. Y. Han and X.-C. Zhang, "Free-space coherent broadband terahertz time-domain spectroscopy," *Meas. Sci. Technol.*, vol. 12, pp. 1747–1756, 2001.

[4] P. H. Bolivar *et al.*, "Measurement of the dielectric constant and loss tangent of high dielectric-constant materials at terahertz frequencies," *IEEE Trans. Microw. Theory Tech.*, vol. 51, no. 4, pt. 1, pp. 1062–1066, Apr. 2003.

[5] M. C. Beard *et al.*, "Subpicosecond carrier dynamics in low-temperature grown GaAs as measured by time-resolved terahertz spectroscopy," *J. Appl. Phys.*, vol. 90, pp. 5915–5923, 2001.

[6] A. Quema *et al.*, "Identification of potential estrogenic environmental pollutants by terahertz transmission spectroscopy," *Jpn. J. Appl. Phys.*, vol. 42, pp. L932–L934, 2003.

[7] Y. Watanabe *et al.*, "Component analysis of chemical mixtures using terahertz spectroscopic imaging," *Opt. Commun.*, vol. 234, pp. 12–129, 2004.

[8] H. Harde *et al.*, "THz time-domain spectroscopy on ammonia," *J. Phys. Chem. A*, vol. 105, pp. 6038–6047, 2001.

[9] G. Zhao *et al.*, "Design and performance of a THz emission and detection setup based on a semi-insulating GaAs emitter," *Rev. Sci. Instrum.*, vol. 73, pp. 1715–1719, 2002.

[10] H. Eisele, M. Naftaly, J. R. Fletcher, D. P. Steenson, and M. R. Stone, "The study of harmonic-mode operation of GaAs TUNNETT diodes and InP Gunn devices using a versatile terahertz interferometer," presented at the 15th Int. Symp. Space Terahertz Technology, Northampton, MA, 2004.

[11] C. McIntosh, J. Toulouse, and P. Tick, "The Boson peak in alkali silicate glasses," *J. Noncrystal. Solids*, vol. 222, pp. 335–341, 1997.

[12] T. Ohsaka and S. Oshikawa, "Effect of OH content on the far-infrared absorption and low-energy states in silica glass," *Phys. Rev. B*, vol. 57, pp. 4995–4998, 1998.

[13] L. Givelder and W. A. Phillips, "Far infrared absorption in disordered solids," *J. Noncrystal. Solids*, vol. 109, pp. 280–288, 1989.

[14] T. J. Parker, J. E. Ford, and W. G. Chambers, "The optical constants of pure fused quartz in the far-infrared," *Infrared Phys.*, vol. 18, pp. 215–219, 1978.

[15] A. H. Verhoef and H. W. den Hartog, "Infrared spectroscopy of network and cation dynamics in binary and mixed alkali borate glasses," *J. Noncrystal. Solids*, vol. 182, pp. 221–234, 1995.

[16] D. W. Lane, "The optical properties and laser irradiation of some common glasses," *J. Phys. D, Appl. Phys.*, vol. 23, pp. 1727–1734, 1990.

[17] H. Selig, M. Khazan, and I. Wilke, "Optical properties of glasses and ceramics for terahertz technology," presented at the CLEO Europe, Nice, France, 2000, paper CTuK113.

[18] S. Kojima, H. Kitahara, S. Nishizawa, Y. S. Yang, and M. W. Takeda, "Terahertz time-domain spectroscopy of low-energy excitation in glasses," *J. Mol. Struct.*, vol. 744–747, pp. 243–246, 2005.

[19] M. J. Jackson and B. Mills, "Thermal expansion of alumino-alkalisilicate and alumino-borosilicate glasses—Comparison of empirical models," *J. Mater. Sci. Lett.*, vol. 16, pp. 1264–1266, 1997.

[20] U. Strom and P. C. Taylor, "Temperature and frequency dependences of the far-infrared and microwave optical absorption in amorphous materials," *Phys. Rev. B*, vol. 16, pp. 5512–5522, 1977.

[21] U. Strom, J. R. Hendrickson, R. J. Wagner, and P. C. Taylor, "Disorder-induced far infrared absorption in amorphous materials," *Solid State Commun.*, vol. 15, pp. 1871–1875, 1974.

[22] R. Boekenhauer *et al.*, "The glass transition temperature of lithium borosilicate glasses related to atomic arrangements," *J. Non-Crystal. Solids*, vol. 175, pp. 137–144, 1994.

[23] S. O. Kasap, *Electronic Materials and Devices*. New York: McGraw-Hill, 2002, pp. 526–534.

[24] M. I. S. Sastry, S. Mukherjee, and A. S. Sarpal, "Molecular dynamic studies of lubricant related systems—Variable temperature IR spectroscopic studies," *Fuel*, vol. 79, pp. 1833–1841, 2000.

[25] X. Z. Wang and B. H. Chen, "Clustering of infrared spectra of lubricating base oils using adaptive resonance theory," *J. Chem. Inf. Comput. Sci.*, vol. 38, pp. 457–462, 1998.

[26] J. Zieba-Palus and P. Koscielniak, "Differentiation of motor oils by infrared spectroscopy and elemental analysis for criminalistic purposes," *J. Mol. Struct.*, vol. 482–483, pp. 533–538, 1999.

[27] T. Bouhacina, B. Desbat, and J. P. Aime, "FTIR spectroscopy and nanotribolofical comparative studies: Influence of the adsorbed water layers on the tribological behaviour," *Tribol. Lett.*, vol. 9, pp. 111–117, 2000.

[28] J. R. Birch, "The far infrared optical constants of polyethylene," *Infrared Phys.*, vol. 30, pp. 195–197, 1990.

[29] J. R. Birch and E. A. Nicol, "The FIR optical constants of the polymer TPX," *Infrared Phys.*, vol. 24, pp. 573–575, 1984.

[30] J. R. Birch, "The far-infrared optical constants of polypropylene, PTFE and polystyrene," *Infrared Phys.*, vol. 33, pp. 33–38, 1992.

[31] G. W. Chantry *et al.*, "Far infrared and millimeter-wave absorption spectra of some low-loss polymers," *Chem. Phys., Lett.*, vol. 10, pp. 473–477, 1971.

[32] S. Arscott *et al.*, "Terahertz time-domain spectroscopy of films fabricated from SU-8," *Electron. Lett.*, vol. 35, pp. 243–244, 1999.

[33] C. Roman *et al.*, "Terahertz dielectric characterization of polymethacrylimide rigid foam: The perfect sheer plate?" *Electron. Lett.*, vol. 40, no. 19, 2004.

[34] S. Kojima, M. W. Takeda, and S. Nishizawa, "Terahertz time domain spectroscopy of complex dielectric constants of boson peaks," *J. Mol. Struct.*, vol. 651–653, pp. 285–288, 2003.

[35] Y.-S. Jin, G.-J. Kim, and S.-G. Jeon, "Terahertz dielectric properties of polymers," *J. Korean Phys. Soc.*, vol. 49, pp. 513–517, 2006.

ABOUT THE AUTHORS

Mira Naftaly received the B.Sc. and M.Sc. degrees in physics from Technion, Israel, and the Ph.D. degree in physics from Brunel University, U.K., in 1989.

She has carried out research at Loughborough and Brunel Universities, and has been at the University of Leeds, Leeds, U.K., as a Senior Research Fellow since 1996. She has published over 50 papers in journals and conference proceedings. Her current research interests are terahertz spectroscopy and development of terahertz generation/detection systems.

Robert E. Miles (Member, IEEE) received the B.Sc. degree in physics from Imperial College London, U.K., in 1964, and the Ph.D. degree from the University of London External Programme, U.K., in 1972.

After leaving university he worked for eight years in the research laboratory of Zenith Radio Research (U.K.) Ltd. This was followed by a further period of about eight years as a school teacher. He then joined the University of Leeds, Leeds, U.K., as a Research Engineer and after a two-year appointment at the University of Bradford, he returned to Leeds in 1981. He became Professor of Electronic Devices at the University of Leeds in 2003. He has published over 90 publications in refereed journals and coedited four books on microwave engineering, semiconductor device modeling, and terahertz technology. His research interests have been in the area of high-frequency electronics and semiconductor devices.